

$$w = \varepsilon w_{(0)}^{(1)} + \varepsilon \kappa w_{(1)}^{(1)} \quad (4.2)$$

along with (2.8), (2.11)-(2.14), (3.10), (3.11), (3.13), (3.14) determine the approximate solution of the problem (1.1)-(1.6). The solution [with use of (1.1)] satisfies (1.3), (1.5), and (1.6) exactly and (1.2) and (1.4) approximately, to within terms small in comparison with  $\varepsilon \kappa$ .

Note that according to (1.1), (2.8), and (4.1), the gas bubble is a sphere and  $S$  is the position vector to the center of the bubble. Using (3.11), (3.14), and (4.2), we find

$$S = \left( \text{Real} \sum_{m=1}^{\infty} S_m e^{2m\pi i t/T} + \bar{W} t \right) \mathbf{k} + S_0, \quad (4.3)$$

where  $S_m = A_0 \varepsilon (w_m + \kappa w_m') / (2m\pi i)$ ;  $\bar{W} = (A_0/T) \varepsilon \kappa \bar{w}$ ;  $S_0$  is constant. The dependence of  $S$  on  $t$  is determined approximately by (4.3). In particular, it follows from (4.3) that the gas bubble moves along a straight line parallel to the  $Z$  axis and its motion is composed of a vibration and a displacement in the direction  $\mathbf{k}$  (for  $\bar{W} > 0$ ) or  $-\mathbf{k}$  (for  $\bar{W} < 0$ ). Hence, vibrations of the liquid (time variation of the velocity and pressure of the liquid) can induce a nonzero average displacement of the bubble. The cause of this displacement is the fact that the conditions for motion of the bubble up and down the axis of vibration of the container are not identical.

#### LITERATURE CITED

1. H. H. Bleich, "Effect of vibrations on the motion of small gas bubbles in a liquid," *Jet Propulsion*, 26, No. 11 (1956).
2. E. Rubin, "Behavior of gas bubbles in vertically vibrating liquid columns" *Can. J. Chem. Eng.*, 46, No. 3 (1968).
3. Foster, Botte, Barbin, and Vakhon, "Bubble trajectories and equilibrium levels in vibrating liquid columns," *Trans. Am. Soc. Mech. Eng., Ser. D, J. Basic Eng.*, 90, No. 1 (1968).
4. Yu. L. Yakimov, "Effect of selective size-dependent drift of gas bubbles in a vibrating liquid," *Izv. Akad. Nauk SSSR, Mekh. Zhidk. Gaza*, No. 4 (1978).
5. G. N. Puchka, "Motion of finely dispersed inclusions in a vibrating container with a liquid containing a compressible sphere," *Prikl. Mekh.*, 17, No. 6 (1981).

#### FLOW STRUCTURE OF A ROTATING LIQUID AFTER MOTION OF A BODY IN IT

V. G. Makarenko and V. F. Tarasov

UDC 532.527

We report the results of an experimental study of the flow structure of a column of liquid which is initially rotating rigidly, after a body is pulled through it in a direction parallel to the axis of rotation. It is shown that the general qualitative result of the motion of the body through the rotating liquid is the formation of a system of cyclone and anticyclone vortices with oscillatory motion of the liquid in them. The properties of these vortices match those reported in [1].

The experimental apparatus is shown schematically in Fig. 1. A transparent vertical cylindrical container 5, in which a liquid rotates with a constant angular velocity  $\omega$ . The motion of the initially rigidly rotating liquid is perturbed by one or several bodies 6 which rotate with the container and complete one pass through the liquid from the bottom of the container to the free surface of the liquid 3 in a direction parallel to the axis of rotation. Thin (0.5 mm) plates in the shape of a circle or a section of a circle were used as the bodies. The plates were mounted parallel to the bottom on thin rods 4 of identical length, which were attached to the disk 2 above the free surface of the liquid. The disk was rotated together with the container and was displaced upward with the help of the rod 1. Until the

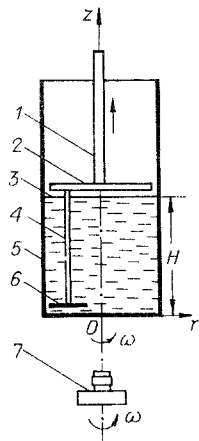


Fig. 1

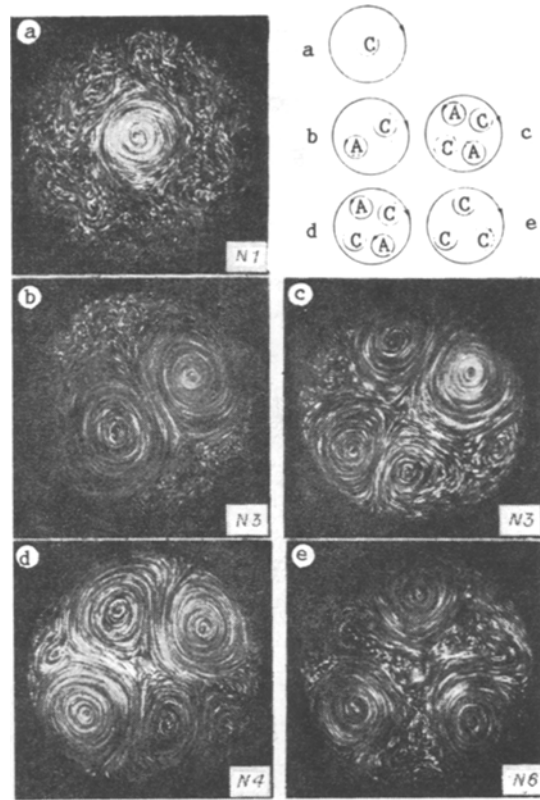


Fig. 2

start of its motion, the body was fixed at 1.5 cm from the bottom of the container. Information on the arrangements, shapes, and sizes of the bodies used in the experiment is given in Table 1.

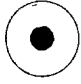






The diameter  $2R$  of the vessel was 18.4 cm. The velocity  $u$  of the body was held constant in any given run and was varied from run to run from 7 to 45 cm/sec. The height  $H$  of the column of liquid in the container was varied from 5 to 35 cm, and the angular velocity of the container was varied from 0.1 to 1.5 rev/sec. The corresponding intervals of Reynolds number  $Re = \omega R^2/\nu$  ( $\nu$  is the kinematic viscosity) and Rossby number  $Ro = u/\omega R$  were  $5 \cdot 10^3 - 8 \cdot 10^4$  and 0.25-1.54, respectively.

The flow fields induced in the liquid after the body was pulled through it were observed visually and recorded photographically. Particles of different buoyancies were used to make the flow field visible. Water or aqueous salt solutions were used as the liquids. The density of the solution was chosen to be equal to the density of the particles in order to ensure neutral buoyancy of the particles.

A system of cyclone and anticyclone vortices was visible for one to two periods of revolution of the container after pulling the body through the rotating liquid. The vortices extended over the entire depth of the liquid and their axes were parallel to the axis of rotation of the container. Oscillatory motion of the liquid inside the vortices was typical. The axial velocity at an arbitrary fixed point on the axis of the vortex was observed to change sign several times during the experiment. The vorticity and axial velocity were observed to oscillate with different amplitudes at different depths inside the vortex. The velocities of the liquid in the cyclone vortices were larger than in the anticyclone vortices, and hence the former were more convenient for visual observation. The vortices can move with respect to the container with a significant azimuthal velocity.

Photographs of different systems of vortices are shown in Fig. 2. To obtain these photographs the flow was made visible using neutrally buoyant polystyrene spheres of diameter 0.5-1 mm and density  $\rho = 1.05 \text{ g/cm}^3$ . The flow field at half height of the column of liquid was illuminated by a plane horizontal beam of width 1 cm. Tracks of particles moving within the illuminated layer were exposed on the film. A camera 7 (see Fig. 1) with shutter speed 0.5 sec mounted on the rotating container was used to take the photographs. The vessel was

TABLE 1

Arrangement No.	Arrangement of the bodies (viewed from above)	Diameter of the disk or circular arc,	Distance between the disk and container axes	Angle of the section of the circle, degrees
		cm		
1		7	0	—
2		13	2,5	180
3		7	5,6	—
4		7	5,6	—
5		18	—	90
6		5	6,6	—
7		18	—	60

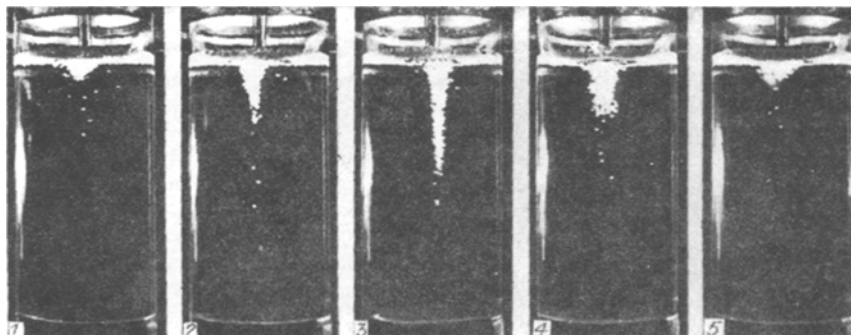


Fig. 3

rotated clockwise with respect to the exposures shown here. In all of these experiments the depth of the liquid in the container, the velocity of the bodies, and the rotational frequency of the body were held constant:  $H = 10$  cm,  $u = 25$  cm/sec,  $\omega = 0.66$  rev/sec. Schematic diagrams indicating the direction of rotation of the large vortices and the container are shown in the upper right corner of Fig. 2. Cyclone vortices are denoted by the letter C and anticyclone vortices by the letter A. The numbers labeling the photographs correspond to the numbers of the arrangements of the bodies listed in Table 1. The flow fields shown in Fig. 2, b-e are also generated after pulling bodies 2, 2, 5, 7, respectively, (see Table 1) through the liquid.

The number of vortices observed in a given experiment can vary during the evolution of the flow field. After motion in the liquid of a disk whose axis is displaced from the axis of symmetry (arrangement 3 in Table 1), two vortices (cyclone and anticyclone; see Fig. 2b) are observed in the early stages of evolution of the flow (after two revolutions of the container). In the later stages of the flow (after 11 revolutions of the container) four large vortices are visible (two cyclones and two anticyclones; see Fig. 2c). Visual observation of the cyclone vortices in these experiments showed that the oscillations of the liquid in them were of the opposite phase. Four large vortices are also observed in Fig. 2d, but in this case the oscillations of the liquid in the two cyclone vortices are in phase with one another. The same is true for the vortices of Fig. 2e. Pairwise fusion of vortices was

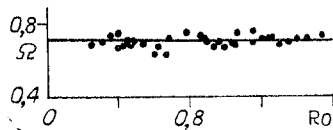


Fig. 4

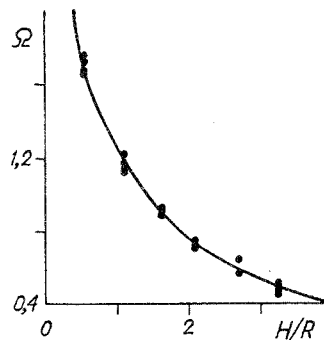


Fig. 5

observed in separate experiments with a large number of cyclone vortices. The amplitudes of the axial velocity and vorticity oscillations in the vortices damp out with time. The oscillations of the liquid in the vortices shown in Fig. 2 were observed over about 20 revolutions of the container.

When a disk whose axis is along the axis of rotation of the container (arrangement 1 of Table 1) is pulled through the rotating liquid, a cyclone vortex is formed near the axis of the flow field. The oscillatory nature of the motion of the liquid in the vortex is illustrated in Fig. 3, in which the photographs show the evolution of the visible "funnel" of the vortex. Exposures were made every 0.4 sec, and  $H = 35$  cm,  $u = 34$  cm/sec,  $\omega = 0.77$  rev/sec. Buoyant polyethylene granules with average diameter 3 mm ( $\rho = 0.92$  g/cm<sup>3</sup>) were used to make the flow visible. Photographs 1 and 2 show that buoyant particles initially at the free surface are drawn downward by the axial flow into the vortex. The maximum length of the "funnel" of the vortex is shown on the third exposure. At this instant of time the maximum vorticity is reached at  $z = H$ ; it is a minimum at  $z = 0$ . Photographs 4 and 5 illustrate the next half-period of the oscillation, in which particles in the vortex are transported upward by the axial flow. In the case where denser-than-water particles are used to make the flow visible the same evolution of the "funnel" is observed, but at the bottom of the container rather than at the surface of the water.

To obtain information on the frequency of the oscillations in the cyclone vortex formed using arrangement 1, a timer was used to record the time  $T$  between successive changes of sign of the axial velocity in the vortex at the half-height level of the liquid column. These times were averaged over 25 oscillations. The dimensionless experimental frequency  $\Omega = 2\pi/\omega T$  is shown by the points on Figs. 4 and 5 as a function of  $Ro$  (for  $H/R = 2.18$ ,  $Re = 2.7 \cdot 10^4$ ) and  $H/R$  (for  $Ro \approx 1$ ,  $Re = 2.7 \cdot 10^4$ ).

Visual observation of this flow field showed that it is identical to the flow described in [1]. The similarity of the flow fields appears in the similarity of their general structure, in the presence of vortices and in the same features and behavior of these vortices.

Normal inertial modes of oscillation were excited in a rotating column of liquid by a resonance method in [1]. The induced flow was the result of resonant "pumping" of a single mode and the flow was observed to retain some of the features of the mode. Vortices were formed in the regions of maximum vertical velocity of the linear mode. The flow field was observed to split up into vertical sections whose length was equal to half the wavelength of the linear mode. The oscillation frequency of the liquid in the vortices was approximately equal to the frequency of the linear mode.

The frequencies measured in our experiments were compared with the frequencies of the linear modes. The curves in Figs. 4 and 5 show the dimensionless frequency of the mode (0, 1, 1) (the first number is the number of periods in the azimuthal angle; the second is the number of zeroes of the radial velocity in the interval  $0 < r \leq R$ , and the third is the number of half-wavelengths along the axis of the container; detailed information on the inertial modes of a rotating liquid in a cylindrical container can be found in [2, 3]). Obviously in this case the experimental frequency  $\Omega$  closely agrees with the frequency of this mode. Observations showed that at large  $Ro$  a significant vertical displacement of particles into the vortex also took place at the same frequency. Hence in the basic features of its structure, the flow observed here is equivalent to the flow induced by resonant excitation of this mode. For small  $Ro$ , the cyclone vortex and its oscillation became less intense the more significant the admixture of high-frequency oscillations. As a critical Rossby number,

above which the low-frequency oscillation will dominate, we can take  $Ro_* = c/\omega R$  ( $c$  is the maximum phase velocity of the axisymmetric wave:  $c = 0.52\omega R$  [4]).

The experimental results show that the vortices were created by the normal inertial oscillations, as in [1]. The only difference is that in [1] the oscillation was excited by resonant "pumping" of effectively a single mode, whereas the flow generated after pulling bodies through the rotating liquid in general has the features of a large number of modes differing in geometry and frequency. This was graphically shown by experiments in which disks of diameter 5 and 10 cm were pulled along the axis of the container at large  $Ro$ . A sharply defined beat was observed at the cyclone vortex generated in the region near the axis. The experimental frequency  $\Omega$  was close to half the sum of the frequencies of the modes (0, 1, 1) and (0, 2, 1) and was lower than for a disk of diameter 7 cm.

Finally we note that, for the intervals of the parameters studied in our experiments, the flow field did not depend on  $Re$ .

#### LITERATURE CITED

1. V. G. Makarenko and V. F. Tarasov, "Experimental model of a tornado," *Zh. Prikl. Mekh. Tekh. Fiz.*, No. 5 (1987).
2. Lord Kelvin, "Vibrations of a columnar vortex," *Philos. Mag.*, 10 (1880).
3. Kh. Grinspen, *Theory of Rotating Fluids* [in Russian], Gidrometeoizdat, Leningrad (1975).
4. G. K. Batchelor, *An Introduction to Fluid Dynamics*, Cambridge University Press (1973).

#### VARIOUS APPROXIMATIONS IN THE THEORY OF CAVITATION FLOWS OF A VISCOUS CAPILLARY FLUID

E. L. Amromin, A. V. Vasil'ev, and V. V. Droblenkov

The purpose of calculating cavitation flows is usually the search of cavity sizes and pressure distributions over streamlined bodies. Most of these calculations are carried out within mechanics of an ideal fluid. However, a number of experimental facts – the presence of a separation boundary layer [1] and a dilatation zone [2] on the body in front of the cavity, the effect of body sizes and its stream velocity on hydrodynamic reactions, cavity sizes [3, 4], and even their existence – require study of the effect of the viscosity of the fluid and its surface tension on cavitation streamline flows of various types.

The pressure diagram for a body with a cavity is determined by the external inviscid flow. The presence of viscosity leads to substantial deviation of the current line from the surfaces of the body and the cavity in three zones: in front of the cavity, behind it, and near the intake extremity of the body. The pressure diagram at the body within these zones also differs substantially from the pressure diagram at a body with a cavity in an ideal fluid. The feature flows in the first two zones are illustrated by Fig. 1: curves 1 and 2 are the cavity boundaries in an ideal and in a viscous capillary fluid for the same  $\sigma$  value – the cavitation number; 3 and 4 are the corresponding calculated pressure diagram coefficient  $C_p$  at the streamline of a body with a cap [1], part of whose meridional cross section contour is illustrated by curve 5;  $\sigma = 2(p_\infty - p_c)\rho^{-1}V_\infty^{-2}$ ;  $C_p = 2(p - p_\infty)\rho^{-1}V_\infty^{-2}$ ;  $\rho$  is the fluid density,  $V_\infty$  is the flow velocity;  $p_\infty$  is the pressure in it; and  $p_c$  and  $p$  are the pressures in the cavity and at an arbitrary point of the boundary between the inviscid and viscous flows. Curves 1-4 are the calculated ones, with  $\sigma = 0.36$ . For an ideal fluid the calculations were carried out by using the generalized Ryabushinskii scheme with closure of the cavity frequency at the edge (whose meridional cross section is illustrated by segment 6), as was done numerically in [3]. For a viscous capillary fluid the calculations were carried out by the method used in [5] for values of the Reynolds number  $Re = 10^6$  and a Weber number  $We = 2 \cdot 10^5$  for vanishing value of the boundary angle, i.e., for an absolutely wetttable body;  $Re$  and  $We = \rho V_\infty^2 D \gamma^{-1}$  are constructed by the same characteristic size  $D$  (the diameter of a

---

Leningrad. Translated from *Zhurnal Prikladnoi Mekhaniki i Tekhnicheskoi Fiziki*, No. 6, pp. 117-126, November-December, 1988. Original article submitted August 20, 1987.